

Highly Active Calcium Oxide Derived from Scallop Shell for Used Cooking Oil Transesterification Reaction



Wiyanti Fransisca Simanullang^{1,2}, Shinya Yamanaka^{3*}

¹ Research Center for Chemistry, National Research and Innovation Agency, Gedung BJ Habibie, Jalan M.H. Thamrin, No. 8, Jakarta Pusat 10340, Indonesia

² Department of Chemical Engineering, Widya Mandala Surabaya Catholic University, Jalan Dinoyo 42-44, Surabaya 60265, Indonesia

³ College of Environmental Technology, Muroran Institute of Technology, Mizumoto-cho 27-1, Muroran 050-8585, Japan

Corresponding Author Email: syama@mmm.muroran-it.ac.jp

<https://doi.org/10.18280/ijdne.170611>

ABSTRACT

Received: 13 August 2022

Accepted: 8 November 2022

Keywords:

liquid additive, grinding, calcium oxide

The liquid additive grinding method was used to improve the specific surface area (SSA) of calcium oxide (CaO) derived from scallop shells as a sustainable resource. Grinding was carried out using a planetary ball mill on a laboratory scale by stepwise addition of some polar and non-polar solvents to determine CaO grinding limit. The crystalline phase of CaO was determined by using X-ray Diffraction (XRD) and SSA was observed based on Brunauer, Emmet, and Teller (BET) method. The mechanism of grinding was obtained from the Scanning Electron Microscope (SEM). The SSA of CaO was increased in proportion to the amount of the liquid additive and grinding time up to 102 m² g⁻¹ while the CaO phase was retained even after the addition of liquid according to the spectra of Fourier Transform-Infrared (FT-IR). The high conversion of triglyceride from used cooking oil to fatty acid methyl esters (FAMES) up to 99% was obtained within an hour at 65°C.

1. INTRODUCTION

The world's demand for energy that is sustainable and environmentally friendly was increased with the increase of the human population and the global warming effect. As a renewable energy source to replace conventional fossil fuels, the development of biodiesel from vegetable oil has been necessary for the global fuel market. The fatty acid methyl ester (FAME) was obtained from the transesterification process of triglyceride in the presence of a catalyst. The catalysts existence becomes a significant role since it affects energy needed and cost production [1-6].

Many research studies have been carried out using CaO as a heterogeneous catalyst because of its high basicity and naturally available i.e. dolomite, limestone, calcite, and shell from marine life [7, 8]. However, CaO from natural resources has a low catalytic activity due to its characteristics such as low solubility, low SSA, and unstable. Therefore, it is recommended to enhance its catalytic activity [9, 10].

The grinding method is one of the promising methods to enhance the catalytic activity of the natural CaO. Dry grinding using liquid additive was satisfactorily effective to increase the grinding efficiency since it helps the ability of the particle to flow accordingly during the grinding process [11-14]. The effect of the grinding aid in this case liquid additive is to shorten the grinding process so that the energy might be decreased [15-20].

In this present study, we tried to treat CaO-based scallop

shell waste which is one of the highest food wastes in Japan as a source of the heterogeneous catalyst. The grinding method was used along with the liquid additive as a grinding aid which was added stepwise into the system. The liquid additive grinding method with liquid additive as a grinding aid to improve the characteristic of CaO-based scallop shell to be high SSA, high, basicity, and high solubility to enhance its catalytic performance on triglyceride conversion to FAME.

2. MATERIAL AND METHODS

2.1 Liquid additive CaO grinding

2.1.1 Materials

The scallop shell powder used in this work was purchased from Tokoro-Cho Industry Promotion Public Corporation (Kitami, Japan). The powder contains >96% calcite. Table 1 lists the chemical composition according to the manufacturer [21]. The specific surface area of the powder before grinding is 1.5 m²g⁻¹ with ρ_p , 2,440 kgm⁻³. The grinding experiments were carried out by a planetary ball mill (Fritsch P-7 premium line, Germany) which was utilized with two zirconia pots (80 cm³ volume and diameter of 39.95 mm) containing 100 g of yttria-stabilized zirconia beads with diameter 3.0 mm was used as the grinding media. The milling beads contain 95% zirconia and 5% yttria with density, ρ_{ball} , 5,950 kgm⁻³ based on the manufacturing company (Nikkato Corporation, Japan).

Table 1. Chemical composition of scallop shell

CaO (%)	Na (%)	MgO (%)	P ₂ O ₅ (%)	K ₂ O (%)	Fe (mg kg ⁻¹)	Mn (mg kg ⁻¹)	Cu (mg kg ⁻¹)	Zn (mg kg ⁻¹)
55.34	0.32	0.14	0.09	0.006	46.8	7.7	2.7	2.2

2.1.2 Methods

A desired amount of CaO was first calcined at 1273 K for 3 h and a liquid additive was added to each pot filled with grinding media. The stepwise addition was conducted in a closed system during the grinding process. The stepwise addition involves adding small amount of tertiary butanol (0.5 g) as a grinding aid to the pot at a predetermined interval (every 1 h) under the grinding conditions shown in Table 2. To evaluate and compare the grinding performance, some other liquid additives i.e., acetone, methanol, ethanol, diethyl ether, benzene, n-hexane, and cyclo-hexane were tested in a similar trend with tertiary butanol. These additives were high-grade reagents (concentration $\leq 100\%$) and were used without further purification.

Table 2. Grinding conditions

Pot volume, V	10 ⁻⁶ m ³	80
Mass of balls, W_B	10 ⁻³ kg	100
Ball-filling ratio, J^a	-	0.35
Ball diameter	10 ⁻³ m	3.0
Sample weight, W_s	10 ⁻³ kg	10.0
Sample loading ratio, U^b	-	0.36
Grinding aid	10 ⁻³ kg	5wt%
Revolution speed	rpm	900
Rotational speed	rpm	900
Grinding time	h	1-over grinding limit

$$^a J = [W_B / \{ \rho_{ball} \times (1 - 0.4) \}] / V, \quad ^b U = (W_s / \rho_p) / (0.4 \times J \times V)$$

The ground mixture was removed after several times of grinding. The BET method (Microtrac, Adsotrac DN-04) with the five-point of measurement was used to determine the SSA of the powder. Five data points in the P/P₀ range 0.025 to 0.30 used to determine the surface area using the BET equation with a positive slope of graph. Degassing powder before the measurement is required under a vacuum for 2 h at 473 K.

Fourier-transform infrared (FTIR) spectra were recorded to determine the powder active site using a JASCO FTIR-460 PlusK spectrometer with KBR pellets. The range of measurements was 4000-400 cm⁻¹ with a resolution of 4 cm⁻¹.

To determine the crystal phase, X-ray diffraction (XRD) was employed using Multi Flex-120 NP Rigaku, Japan with Cu K α (wavelength $\lambda = 1.5418 \text{ \AA}$). The measurements operated at radiation 40 kV and 20 mA. The powder patterns were recorded with 0.02° step size over the 2 θ in a range of 3-70° at room temperature. Crystalline phases of the powder were identified by comparison with ICDD data files.

The mechanisms of grinding were studied using a scanning electron microscope (SEM) analysis by JEOL JSM 6380 A with 20 keV voltage. The sample powder was covered in a carbon film with a certain magnification for capturing.

The total basic sites (fm) of the catalysts from the acidity conjugate acid were determined by the titration method. In the typical experiments, 25 mg CaO was dissolved in an HCl solution (25 mL; 0.1 M) and stirred for 1 h. The HCl solution will be neutralized by the catalyst which is equivalent to its basicity. The resulting solution was titrated against standard NaOH solution to determine the concentration of excess HCl

when the color of the solution was changed from colorless to soft pink in the presence of a phenolphthalein indicator. The amount of HCl neutralized by the catalyst is the representation of the catalyst basicity as mmol of HCl/g of catalyst [22].

2.2 CaO grinding catalytic activity on transesterification of used cooking oil

2.2.1 Materials

The free fatty acid (FFA) of used cooking oil was analyzed by a standard titration. Before titration, a certain amount of sample (~5g) was dissolved in 10 g ethanol and warmed at 67°C. The pH change was determined by phenolphthalein indicator during titration with KOH 0.1 M, according to the equation given below:

$$A = [\text{KOH}] \times v \text{ KOH} \times \text{Mr OA} / \text{m sample} \quad (1)$$

where,

[KOH] = concentration of KOH solution (M);

v KOH = volume of KOH solution (L);

Mr OA = molecular weight (g mol⁻¹).

$$\% \text{FFA} = A / 2 \quad (2)$$

In Eq. (1) the subscript OA refers to the oleic acid which is a type of FFA while the water content of UCO was measured by using the centrifuge method (900 rpm in ten minutes) repeatedly until the water content was completely removed. The FAME yield (%) was calculated by using Eq. (3) according to reference [23].

$$\text{Yield (\%)} = \frac{m_i A_b}{A_i m_b} \times 100 \quad (3)$$

where,

m_i = mass of internal standard,

A_i = peak area of internal standard,

m_b = mass of the sample,

A_b = peak area of the sample. The water content of UCO was measured based on a method in the literature [24].

2.2.2 Method

Transesterification of used cooking oil (FFA=31% and water content = 2%) with methanol was carried out in a three-necked glass flask with a magnetic stirrer connected to a condenser. Transesterification reactions were performed at 65±1°C with a molar ratio of oil to methanol 1:9 and catalyst concentration of 2wt% and stirring at 900 rpm. FAMES conversion was analyzed using a flame ionization detector (FID) gas chromatograph (Shimadzu GC-14B), on a DB-5HT capillary column (14 m×0.25 mm, 0.1 μm film thickness). The analytical work was performed with the following heating regime: holding at 50°C for 1 min, followed by three separate steps of temperature increase, firstly to 180°C at a rate of 10°C/min, then to 230°C at 7°C/min, and lastly, to 380°C at 10°C/min, at which point the temperature was held for 10 min.

3. RESULT AND DISCUSSION

3.1 Liquid additive CaO grinding

The XRD patterns of CaO in the scallop shell (Figure 1) showed that the CaO phase remained even after liquid additive grinding treatment (ICDD file 04-1497), indicating that the liquid additive did not change the CaO active site.

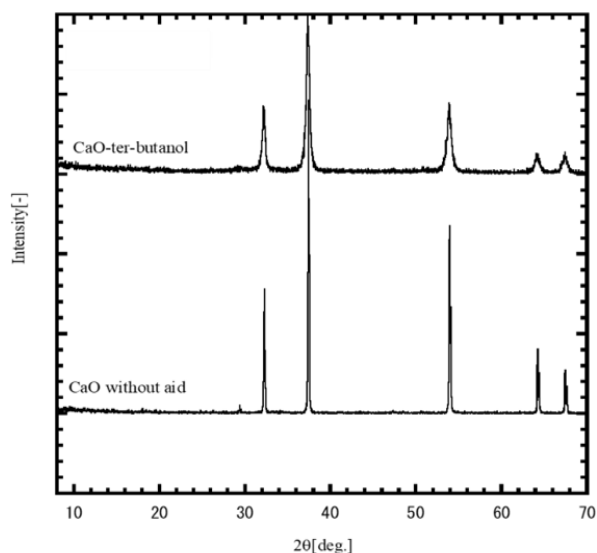


Figure 1. XRD pattern of CaO grinding

SEM pictures of CaO support the XRD measurement. After grinding for several hours with and without additives (Figure 2). SEM pictures showed that the grinding process with liquid additives breaks the bulk material into small CaO particles which indicates that liquid additives were absorbed on the surface to decrease the surface energy [25].

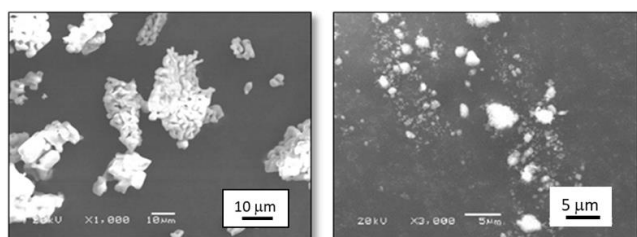


Figure 2. Scanning Electron Microscope (SEM) pictures of (a) CaO scallop shell (b) CaO liquid additive grinding

The grinding process could promote by the chemisorption of liquid additives to increase the flow ability during grinding on the surface of particles. Overall, the average size becomes progressively smaller with time as shown in Figure 3a and 3b. However, the excessive liquid additives tend to make the CaO powder agglomerate over the grinding limit as shown in Figure 3c and 3d. This finding supports the grinding mechanism (Figure 4) have been mentioned in literature so-called attrition and breakage [26-28].

Liquid additive CaO grinding enhance not only the SSA of CaO from $1.5 \text{ m}^2\text{g}^{-1}$ up to $100 \text{ m}^2\text{g}^{-1}$ but also the grinding efficiency (Figure 5). The specific surface area tends to increase and then decrease by the amount of grinding aid and time which leads to the determining of the true grinding limit [29-32]. This process includes the adsorption of the liquid on the surface of CaO. As a result, the surface energy of the solid

CaO decreases, and the grinding process is easy to perform.

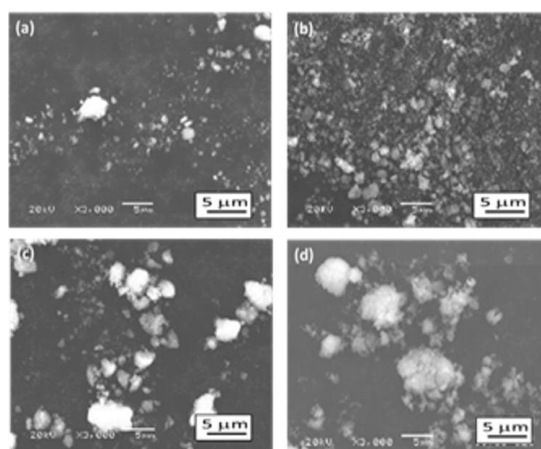


Figure 3. Scanning Electron Microscope (SEM) pictures of (a) 1 h grinding; 0.5 g additives (b) 10 h grinding; 5 g additives (c) 13 h grinding; 6.5 g additives (d) 14 h grinding; 7 g additives

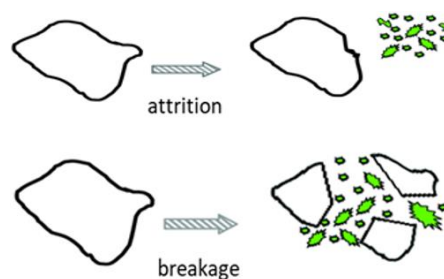


Figure 4. Schemes of the attrition and breakage CaO liquid additive grinding

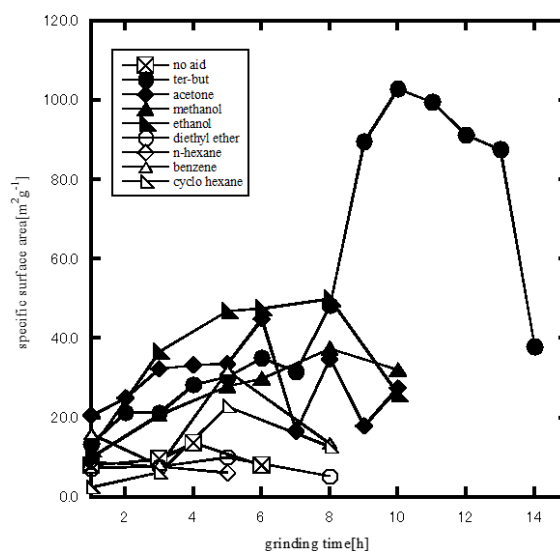


Figure 5. Relationship between the SSA and liquid additive grinding time

The FT-IR spectra of both CaO with and without liquid additive (Figure 6) showed a strong and broadband at 400 cm^{-1} corresponding to CaO which indicates that the surface of CaO was retained even after grinding. The strong peak at 3642 cm^{-1} is the OH group. A strong -OH peak is characteristic of CaO standard [29]. This result suggests that liquid additive grinding on CaO retains its surface.

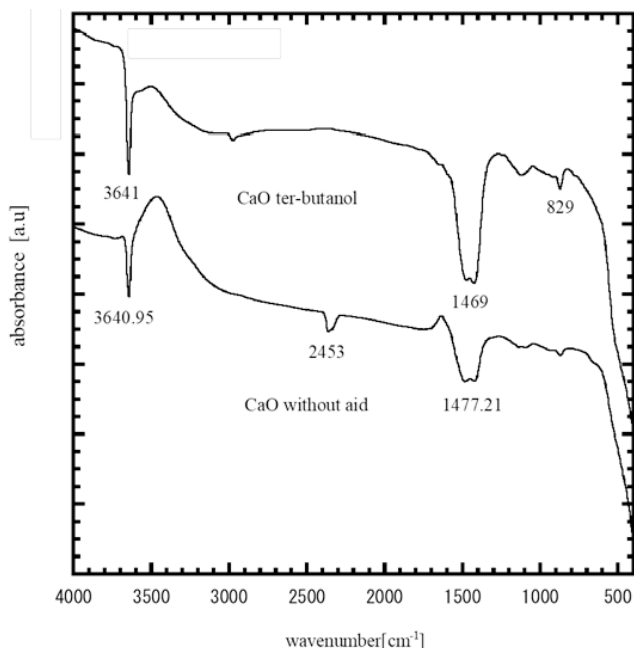


Figure 6. FT-IR spectra of CaO after grinding

3.2 CaO grinding catalytic activity on transesterification of used cooking oil

The catalytic activity on the transesterification reaction of CaO-based scallop shell with liquid additive grinding treatment on used cooking oil with 31% of free fatty acid and 2% water at 65°C within 1 h was shown in Figure 7.

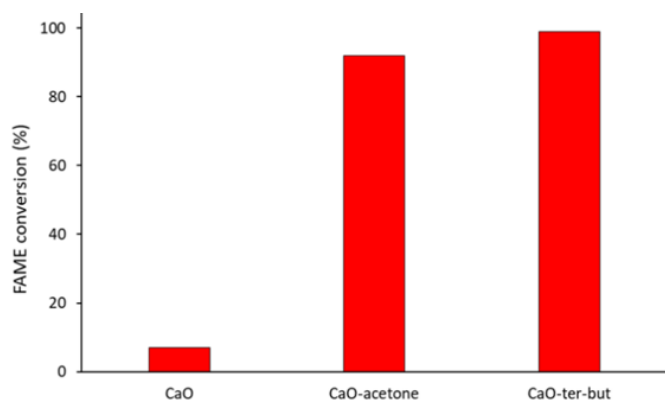


Figure 7. Catalytic performance CaO scallop shell and CaO liquid additive grinding in transesterification of used cooking oil (catalyst loading: 2wt%, T=65°C, t=1h)

Table 3. CaO grinding: SSA, basicity, and FAME yield

Catalyst	SSA (m ² g ⁻¹)	Basicity (mmol g ⁻¹)	FAME yield (%)
CaO	1.5	0.096	7
CaO-acetone	45	0.284	92
CaO-ter-butanol	102.0	0.284	99

Relatively high FAME conversion from triglyceride of used cooking oil reached 92% and 99% for CaO-acetone and CaO-tertiary butanol, respectively while CaO grinding scallop shell reached only 7% conversion. This indicates that the high SSA catalysts obtained from liquid additive grinding are more efficient than the untreated ones (Table 3). Moreover, the stepwise addition of liquid additives during grinding increases

the basicity of the CaO without changing its surface active site. Liquid additive grinding was successfully effective to enhance the catalytic transesterification of CaO derived from a scallop shell.

4. CONCLUSION

Liquid additive grinding was successfully effective to enhance the SSA of the CaO-based scallop shell. The SSA of CaO tends to increase and then to decreased proportionally to grinding time which suggests that the grinding limit was obtained at the maximum SSA=102 m²g⁻¹. Liquid additive retains the surface active site of CaO, hence, the catalytic performance in the transesterification reaction is increased. The controllable active site and high SSA of CaO showed highly active performance in the conversion of a triglyceride of used cooking oil into FAME up to 99% at 65°C within 1 h reaction. However, the stability of the CaO-based scallop shell needs to study further. The obtained insight in this study is a promising approach for developing the scallop shell based catalyst as an environmentally friendly technology for developing the marine waste based catalyst for biodiesel production.

REFERENCES

- [1] Kesic, Ž., Lukic, I., Zdujic, M., Mojovic, L., Skala, D. (2016). Katalizatori na bazi oksida kalcijuma u procesima sinteze biodizela: Presek stanja. *Chemical Industry and Chemical Engineering Quarterly*, 22(4): 391-408. <https://doi.org/10.2298/CICEQ160203010K>
- [2] Marinković, D.M., Stanković, M.V., Veličković, A.V., Avramović, J.M., Miladinović, M.R., Stamenković, O.O., Veljković, V.B., Jovanović, D.M. (2016). Calcium oxide as a promising heterogeneous catalyst for biodiesel production: Current state and perspectives. *Renewable and Sustainable Energy Reviews*, 56: 1387-1408. <https://doi.org/10.1016/j.rser.2015.12.007>
- [3] Miladinović, M.R., Krstić, J.B., Tasić, M.B., Stamenković, O.S., Veljković, V.B. (2014). A kinetic study of quicklime-catalyzed sunflower oil methanolysis. *Chemical Engineering Research and Design*, 92(9): 1740-1752. <https://doi.org/10.1016/j.cherd.2013.11.023>
- [4] Jindapon, W., Jaiyen, S., Ngamcharussrivichai, C. (2016). Seashell-derived mixed compounds of Ca, Zn and Al as active and stable catalysts for the transesterification of palm oil with methanol to biodiesel. *Energy Conversion and Management*, 122: 535-543. <https://doi.org/10.1016/j.enconman.2016.06.012>
- [5] Santri, D.J., Zulkifli, H., Aldes Lesbani, H., Anwar, Y., Ermayanti, V.M., Fudholi, A. (2021). Analysis of swamp microalgal isolates from south Sumatra as biofuel candidates. *International Journal of Design & Nature and Ecodynamics*, 16(6): 625-630. <https://doi.org/10.18280/ijdne.160602>
- [6] Widyaningrum, T., Utami, L.B., Prastowo, I., Meylani, V., Permadi, A. (2022). Comparison of bioethanol production using *Saccharomyces cerevisiae* and *Zymomonas mobilis* in fermented jackfruit peel treated with blend crude cellulose enzymes. *International Journal of Design & Nature and Ecodynamics*, 17(4): 633-637. <https://doi.org/10.18280/ijdne.170420>

- [7] Jaiyen, S., Naree, T., Ngamcharussrivichai, C. (2015). Comparative study of natural dolomitic rock and waste mixed seashells as heterogeneous catalysts for the methanolysis of palm oil to biodiesel. *Renewable Energy*, 74: 433-440. <https://doi.org/10.1016/j.renene.2014.08.050>
- [8] Mahesh, S.E., Ramanathan, A., Begum, K.M.S., Narayanan, A. (2015). Biodiesel production from waste cooking oil using KBr impregnated CaO as catalyst. *Energy Conversion and Management*, 91: 442-450. <https://doi.org/10.1016/j.enconman.2015.02.044>
- [9] Jindapon, W., Ruengyoo, S., Kuchonthara, P., Ngamcharussrivichai, C., Vitidsant, T. (2020). Continuous production of fatty acid methyl esters and high-purity glycerol over a dolomite-derived extrudate catalyst in a countercurrent-flow trickle-bed reactor. *Renewable Energy*, 157: 626-636. <https://doi.org/10.1016/j.renene.2020.05.066>
- [10] Pavlović, S.M., Marinković, D.M., Kostić, M.D., Lončarević, D.R., Mojović, L.V., Stanković, M.V., Veljković, V.B. (2021). The chicken eggshell calcium oxide ultrasonically dispersed over lignite coal fly ash-based cancrinite zeolite support as a catalyst for biodiesel production. *Fuel*, 289: 119912. <https://doi.org/10.1016/j.fuel.2020.119912>
- [11] Chen, X. S., Li, Q., Fei, S. M. (2008). Constrained model predictive control in ball mill grinding process. *Powder Technology*, 186(1): 31-39. <https://doi.org/10.1016/j.powtec.2007.10.026>
- [12] Shi, F., Xie, W. (2015). A specific energy-based size reduction model for batch grinding ball mill. *Minerals Engineering*, 70: 130-140. <https://doi.org/10.1016/j.mineng.2014.09.006>
- [13] Simba, K.P., Moys, M.H. (2014). Effects of mixtures of grinding media of different shapes on milling kinetics. *Minerals Engineering*, 61: 40-46. <https://doi.org/10.1016/j.mineng.2014.03.006>
- [14] Hanumanthappa, H., Vardhan, H., Mandela, G.R., Kaza, M., Sah, R., Shanmugam, B.K. (2020). A comparative study on a newly designed ball mill and the conventional ball mill performance with respect to the particle size distribution and recirculating load at the discharge end. *Minerals Engineering*, 145: 106091. <https://doi.org/10.1016/j.mineng.2019.106091>
- [15] Panjaitan, F.R., Yamanaka, S., Kuga, Y. (2017). Soybean oil methanolysis over scallop shell-derived CaO prepared via methanol-assisted dry nano-grinding. *Advanced Powder Technology*, 28(7): 1627-1635. <https://doi.org/10.1016/j.apt.2016.12.020>
- [16] Mazaheri, H., Ong, H.C., Masjuki, H.H., et al. (2018). Rice bran oil based biodiesel production using calcium oxide catalyst derived from *Chicoreus brunneus* shell. *Energy*, 144: 10-19. <https://doi.org/10.1016/j.energy.2017.11.073>
- [17] Mansir, N., Teo, S.H., Rashid, U., Taufiq-Yap, Y.H. (2018). Efficient waste *Gallus domesticus* shell derived calcium-based catalyst for biodiesel production. *Fuel*, 211: 67-75. <https://doi.org/10.1016/j.fuel.2017.09.014>
- [18] Toraman, O.Y. (2012). Effect of chemical additive on stirred bead milling of calcite powder. *Powder technology*, 221: 189-191. <https://doi.org/10.1016/j.powtec.2011.12.067>
- [19] Hasegawa, M., Kimata, M., Shimane, M., Shoji, T., & Tsuruta, M. (2001). The effect of liquid additives on dry ultrafine grinding of quartz. *Powder Technology*, 114(1-3): 145-151. [https://doi.org/10.1016/S0032-5910\(00\)00290-4](https://doi.org/10.1016/S0032-5910(00)00290-4)
- [20] Hasegawa, M., Kimata, M., Yaguchi, M. (2006). Effect and Behavior of Liquid Additive Molecules in Dry Ultrafine Grinding of Limestone [Translated]. *KONA Powder and Particle Journal*, 24: 213-221. <https://doi.org/10.14356/kona.2006023>
- [21] Yamanaka, S., Suzuma, A., Fujimoto, T., Kuga, Y. (2013). Production of scallop shell nanoparticles by mechanical grinding as a formaldehyde adsorbent. *Journal of nanoparticle research*, 15(4): 1573. <https://doi.org/10.1007/s11051-013-1573-x>
- [22] Kaur, N., Ali, A. (2014). Kinetics and reusability of Zr/CaO as heterogeneous catalyst for the ethanolysis and methanolysis of *Jatropha curcas* oil. *Fuel Processing Technology*, 119: 173-184. <https://doi.org/10.1016/j.fuproc.2013.11.002>
- [23] Jiang, S.T., Zhang, F.J., Pan, L.J. (2010). Sodium phosphate as a solid catalyst for biodiesel preparation. *Brazilian Journal of Chemical Engineering*, 27: 137-144. <https://doi.org/10.1590/S0104-66322010000100012>
- [24] Posom, J., Sirisomboon, P. (2015). Evaluation of the moisture content of *Jatropha curcas* kernels and the heating value of the oil-extracted residue using near-infrared spectroscopy. *Biosystems Engineering*, 130: 52-59. <https://doi.org/10.1016/j.biosystemseng.2014.12.003>
- [25] Sureshan, K.M. (1992). Mechanism of action of grinding aids in comminution. *Powder Technol.*, 71: 229-237. [https://doi.org/10.1016/0032-5910\(92\)88029-H](https://doi.org/10.1016/0032-5910(92)88029-H)
- [26] Hogg, R. (1999). Breakage mechanisms and mill performance in ultrafine grinding. *Powder Technology*, 105(1-3): 135-140. [https://doi.org/10.1016/S0032-5910\(99\)00128-X](https://doi.org/10.1016/S0032-5910(99)00128-X)
- [27] Sohoni, S., Sridhar, R., Mandal, G. (1991). The effect of grinding aids on the fine grinding of limestone, quartz and Portland cement clinker. *Powder technology*, 67(3): 277-286. [https://doi.org/10.1016/0032-5910\(91\)80109-V](https://doi.org/10.1016/0032-5910(91)80109-V)
- [28] Choi, H., Lee, W., Kim, D.U., et al. (2010). Effect of grinding aids on the grinding energy consumed during grinding of calcite in a stirred ball mill. *Minerals Engineering*, 23(1): 54-57. <https://doi.org/10.1016/j.mineng.2009.09.011>
- [29] Marinković, D.M., Avramović, J.M., Stanković, M.V., Stamenković, O.S., Jovanović, D.M., Veljković, V.B. (2017). Synthesis and characterization of spherically-shaped CaO/ γ -Al₂O₃ catalyst and its application in biodiesel production. *Energy Conversion and Management*, 144: 399-413. <https://doi.org/10.1016/j.enconman.2017.04.079>
- [30] Marinković, D.M., Miladinović, M.R., Avramović, J.M., Krstić, I.B., Stanković, M.V., Stamenković, O.S., Jovanović, D.M., Veljković, V.B. (2018). Kinetic modeling and optimization of sunflower oil methanolysis catalyzed by spherically-shaped CaO/ γ -Al₂O₃ catalyst. *Energy Conversion and Management*, 163: 122-133. <https://doi.org/10.1016/j.enconman.2018.02.048>
- [31] Knieke, C., Sommer, M., Peukert, W. (2009). Identifying the apparent and true grinding limit. *Powder Technology*, 195(1): 25-30. <https://doi.org/10.1016/j.powtec.2009.05.007>
- [32] Yu, J., Qin, Y., Gao, P., Han, Y., Li, Y. (2021). An innovative approach for determining the grinding media

system of ball mill based on grinding kinetics and linear superposition principle. Powder Technology, 378: 172-

181. <https://doi.org/10.1016/j.powtec.2020.09.076>